RESEARCH ARTICLE | APRIL 13 2023

Investigating the effect of surface protrusions on galloping energy harvesting

Juntong Xing; Masoud Rezaei; Huliang Dai; ... et. al

Appl. Phys. Lett. 122, 153902 (2023)
https://doi.org/10.1063/5.0142143

Applied Physics Letters ARTICLE scitation.org/journal/apl

Investigating the effect of surface protrusions on galloping energy harvesting

Cite as: Appl. Phys. Lett. **122**, 153902 (2023); doi: 10.1063/5.0142143
Submitted: 11 January 2023 · Accepted: 31 March 2023 ·
Published Online: 13 April 2023

View Online Export Citation CrossMark

Juntong Xing,[1] Masoud Rezaei,[1,2] Huliang Dai,[3] and Wei-Hsin Liao[1,a)]

AFFILIATIONS

[1]Department of Mechanical and Automation Engineering, The Chinese University of Hong Kong, Shatin, New Territories, Hong Kong, China
[2]School of Mechanical Engineering, Iran University of Science and Technology, Narmak, Tehran, Iran
[3]Hubei Key Laboratory for Engineering Structural Analysis and Safety Assessment, School of Aerospace Engineering, Huazhong University of Science and Technology, Wuhan 430074, China

[a)]**Author to whom correspondence should be addressed:** whliao@cuhk.edu.hk. **URL:** http://www.mae.cuhk.edu.hk/~whliao/

ABSTRACT

This Letter explores the potential effect of implementing different surface protrusions on galloping energy harvesters. Three types of protruded bluff bodies with rectangular, triangular, and elliptical metasurfaces are proposed, and four kinds of surface treatments are deployed to vary their protruded shape. Wind tunnel experiments reveal that adding the protrusions can obviously change the mode of oscillations, and only the backward protrusions can enhance the galloping response. Both the experiments and simulations show that elliptical surface protrusions have the greatest potential to enhance the galloping energy harvesting performance. Specifically, with a backward protruded length of 15 mm, the maximum output power in the experiments is measured to be 0.757 mW, which occurs at 5.1 m/s, and an optimal load resistance of 300 kΩ. In this case, the energy harvester outperforms its counterpart carrying a simple square prism by 157.48%.

Small-scale wind energy harvesting has emerged as a promising approach for realizing self-powered wireless sensor networks or Internet of Things (IoT).[1–3] Unlike a large-scale wind energy conversion system, e.g., a wind turbine, which is generally applicable when strong wind is available, this technology can be utilized to scavenge the untapped energy from a gentle or light breeze, which is ubiquitous in environment. Therefore, designing efficient small-scale wind energy harvesters has been an ongoing research topic in recent decades.[4–8]

Flow-induced vibrations, as typical carriers of wind kinetic energy, can be converted to electricity using piezoelectric, electromagnetic, electrostatic, and triboelectric mechanisms.[9–11] Among these, piezoelectric transducers (PZTs) are given special attention because of their higher energy density, ease of implementation, and independency of external voltage input or magnetic field. Flow-induced vibrations can be classified as vortex-induced vibrations (VIVs),[12,13] galloping,[14,15] flutter,[4,16] and buffeting.[5,7] In particular, galloping oscillations have a large vibration amplitude and possess the ability of oscillating in a wide range of wind speeds. Therefore, galloping piezoelectric energy harvesting (GPEH) technology has received a great attention and is used in some cutting-edge designs. Yang *et al.*[17] conducted a comparative study of different cross sections (square, rectangles with various aspect ratios, equilateral triangle, and D-section) of bluff bodies for GPEH. The results revealed that the square-sectioned bluff body outperforms the others with a low cut-in speed of 2.5 m/s and a high peak output power of 8.4 mW. Thereafter, researchers proposed modified designs to enhance energy harvesting performance. Hu *et al.*[18] verified that fitting fins to the leading edge of a square prism can improve the efficiency of GPEH up to 150%. Alhadidi *et al.*[15] proposed a method to improve the sensitivity of GPEH by adding Y-shaped attachments of various lengths and fork angles on the rear face of a square prism. Results manifested that the galloping rise time can be reduced by 75%, compared to the finless square prism.

Integrating metasurfaces into flow-induced energy harvesters is a promising method of improving flow-induced energy harvesting performance. However, a batch of pertinent research exists in the field of VIV. Wang *et al.*[19] for the first time explored the use of metasurfaces for VIV suppression or energy harvesting. It was shown that the existence of metasurfaces can influence the flow field around cylindrical bluff bodies and, hence, alter the generated aerodynamic force. Tang *et al.*[20] further investigated the effect of a metasurface structure on the

enhancement of VIV energy harvesting at the downstream of an interference long cylinder. It was indicated that the larger size of metasurface structures is more conducive to energy harvesting performance improvement at lower wind speeds, and 'V'-shaped metasurface performs the best. Nevertheless, in the field of GPEH, there has been little research on this topic. Only one systematic study conducted by Wang *et al.*[21] manifests that when convex cylinder ornaments (each with a diameter of 6 mm and a length of 9 mm) are attached to a bluff body, the maximum output voltage can be increased by 26.14%. However, it is worth mentioning that all the aforementioned studies are based on full-surface metasurface structures, i.e., the surface modifications are distributed throughout the whole bluff body. No relevant study has been conducted to investigate the potential effect of single-sided metasurfaces on GPEH, which may differ when the surface protrusions are considered on different sides.

In this Letter, with the aim of investigating the potential effect of different surface protrusions on the GPEH performance, three types of protruded bluff bodies (with rectangular/triangular/elliptical metasurfaces) are proposed as shown in Fig. 1(a). For each of the shapes, four kinds of surface treatments, including all-sided, frontal, side, and backward, which are, respectively, depicted from left to right in Fig. 1(a), are considered. The original bluff body, which is a $30 \times 30 \times 70\ \text{mm}^3$ square prism, serves as a reference for the purpose of comparison in further experimental and analytical investigations. Figures 1(b) and 1(c), respectively, present the overall experimental setup and the details of the GPEH system. The proposed energy harvester is composed of a cantilever beam (PLA, $82 \times 20 \times 1\ \text{mm}^3$), a Macro Fiber Composite (MFC) patch (M2814-P2, $28 \times 14 \times 0.33\ \text{mm}^3$, Smart Material Corporation), and a tip bluff body. The whole experimental setup was placed inside the open-circuit wind tunnel, and the output signals were recorded by an oscilloscope (STO1104C, Micsig). The anemometer (testo 405i) was used to measure the wind speed, and the laser sensor (HG-C1100, Panasonic) was mounted parallel to the beam structure to detect its real-time tip deflection. A series of experiments were conducted in the speed range of 0–5.1 m/s, as a simulation of the natural gentle breeze.[22]

Under open-circuit conditions, three types of protruded bluff bodies with four different surface treatments of a fixed protruded length of 5 mm are deployed for an initial forward wind sweep experiment. The beam tip deflection and RMS of generated voltage vs wind speed are plotted in Fig. 2. Based on this figure, the original bluff body experiences galloping oscillations as expected. On the contrary, adding the protrusions affects the mechanical and electrical responses of the GPEH considerably. Specifically, for the backward protrusions, all three protruded shapes (rectangle/triangle/ellipse) can enhance the GPEH performance through improving its response and voltage amplitudes; for the frontal protrusions, the triangular and elliptical shapes can also give rise to galloping, but attenuated, while the rectangular shape cannot. Furthermore, for the side and all-sided protrusions, none of the shapes can lead to galloping, but vortex-induced vibrations, so as to reduce the energy harvesting performance in almost the whole range of the considered wind speeds. Therefore,

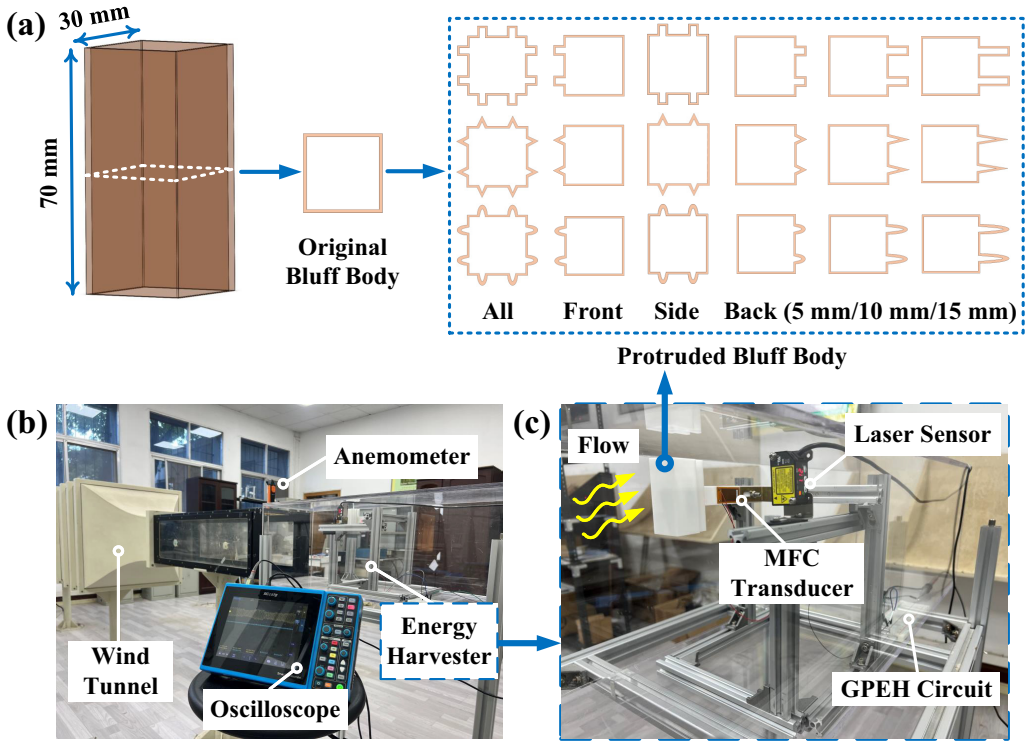

FIG. 1. (a) Schematics of the proposed protruded bluff bodies with different surface treatments; (b) experimental setup; and (c) details of the galloping piezoelectric energy harvesting system.

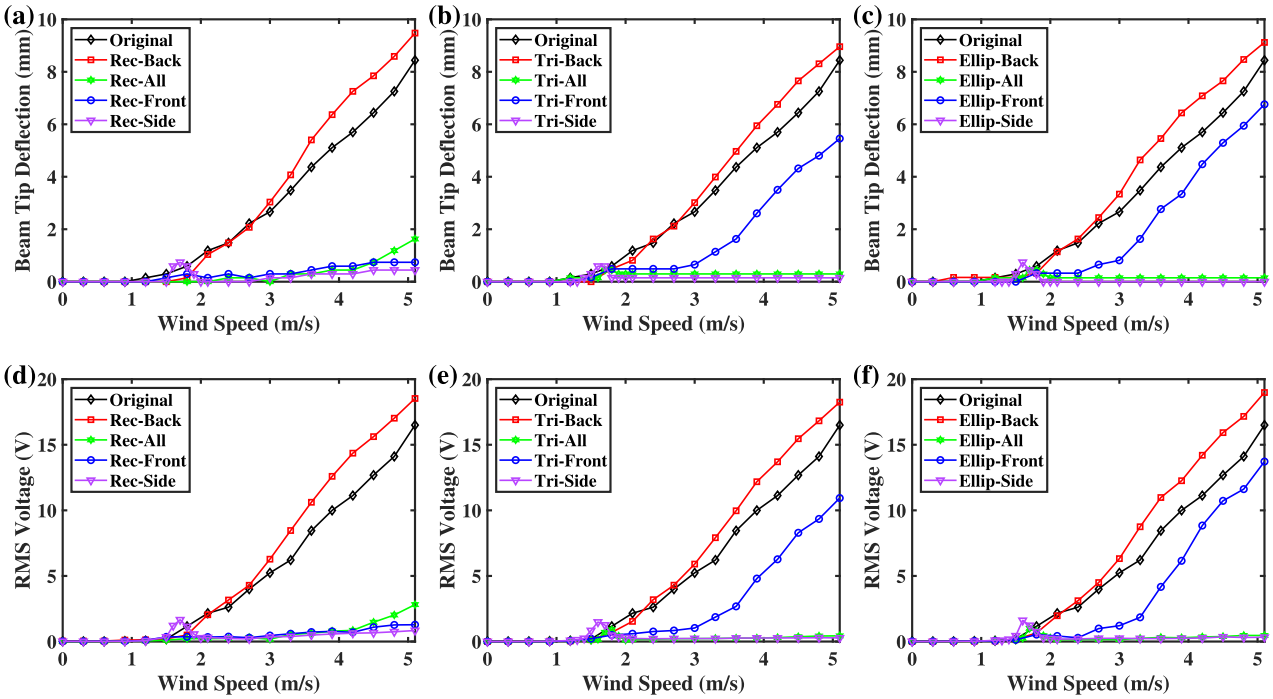

FIG. 2. Experimental dynamic responses of different protruded bluff bodies with a fixed protruded length of 5 mm and height of 70 mm: (a)–(c) Tip deflection of bluff bodies with rectangular, triangular, and elliptical metasurfaces and (d)–(f) RMS voltage of bluff bodies with rectangular, triangular, and elliptical metasurfaces.

based on the results of Fig. 2, the backward protrusions enhance the performance of the proposed GPEH, in comparison with the ordinary GPEH, through increasing the amplitudes of vibrations and harvested voltage. Specifically, under the test speed of 5.1 m/s, the GPEH carrying backward protruded bluff bodies with rectangular/triangular/elliptical metasurfaces outperform the original one by 12.31%, 10.61%, and 15.06%, respectively, in terms of the harvested voltage. Therefore, the finding of this study discloses that backward metasurfaces can enhance the GPEH performance, and this motivates a deeper investigation regarding the influence of different backward protruded lengths. As shown in Fig. 1(a), except the length of 5 mm, two other protruded lengths of 10 and 15 mm are also considered as a comparative study. The experimental results of considering different lengths for backward protrusions are depicted in Figs. 3(a)–3(c). It can be observed that, for each shape of protrusions, the galloping cut-in speed increases slightly as the protruded length increases. At the same time, the galloping oscillations amplitude get amplified at higher wind speeds. Under the highest test speed of 5.1 m/s, the associated harvested voltage of the rectangular/triangular/elliptical backward length of 15 mm outperforms the reference system by 33.03%, 35.97%, and 53.76%, respectively. This implies that elliptical backward protrusions perform the best in terms of the efficiency enhancement of GPEH.

In order to account for the discovered experimental phenomenon, mathematical modeling can be established based on the extended Hamilton's principle[11,23] and Euler–Bernoulli beam theory.[24] The derived governing equations of the proposed GPEH can be described as

$$\begin{cases} m\ddot{w} + c\dot{w} + YIw'''' + YI\{w'(w'w'')'\}' + \left\{\theta\left(1+\frac{1}{2}w'^2\right)\right\}''v \\ \quad = F_a\left(\delta(x-L_b) - \frac{D_b}{2}\delta'(x-L_b)\right), \\ C_p\dot{v} + \frac{1}{R}v = \frac{\partial}{\partial t}\left\{\int_0^{L_b}\theta w''\left(1+\frac{1}{2}w'^2\right)dx\right\}, \end{cases} \tag{1}$$

where w, m, YI, and L_b are the transverse displacement, mass, bending stiffness, and length of the cantilever beam, respectively. Furthermore, c is the dimensional damping of the system, θ is the electromechanical coupling coefficient, C_p is the capacitance, R is the load resistance, and v denotes the output voltage of the PZT circuit. In addition, F_a is the galloping aeroelastic force, which can be expressed as follows:

$$F_a = \frac{1}{2}\rho U_f{}^2 L D_b C_{Fy}, \tag{2}$$

where ρ is the air density and U_f denotes the wind speed. Moreover, L and D_b, respectively, stand for the frontal length and width of the bluff body and C_{Fy} denotes the transverse force coefficient, which can be derived by lift coefficient C_L, drag coefficient C_D, and the angle of attack α (AoA). Using a third order polynomial approximation,[14] C_{Fy} can be explicitly expressed as a function of the AoA as[25,26]

$$C_{Fy} = -(C_L + C_D\tan\alpha)\sec\alpha \approx A_1\alpha - A_3\alpha^3. \tag{3}$$

Furthermore, according to the relationship between AoA and beam deflection,[11]

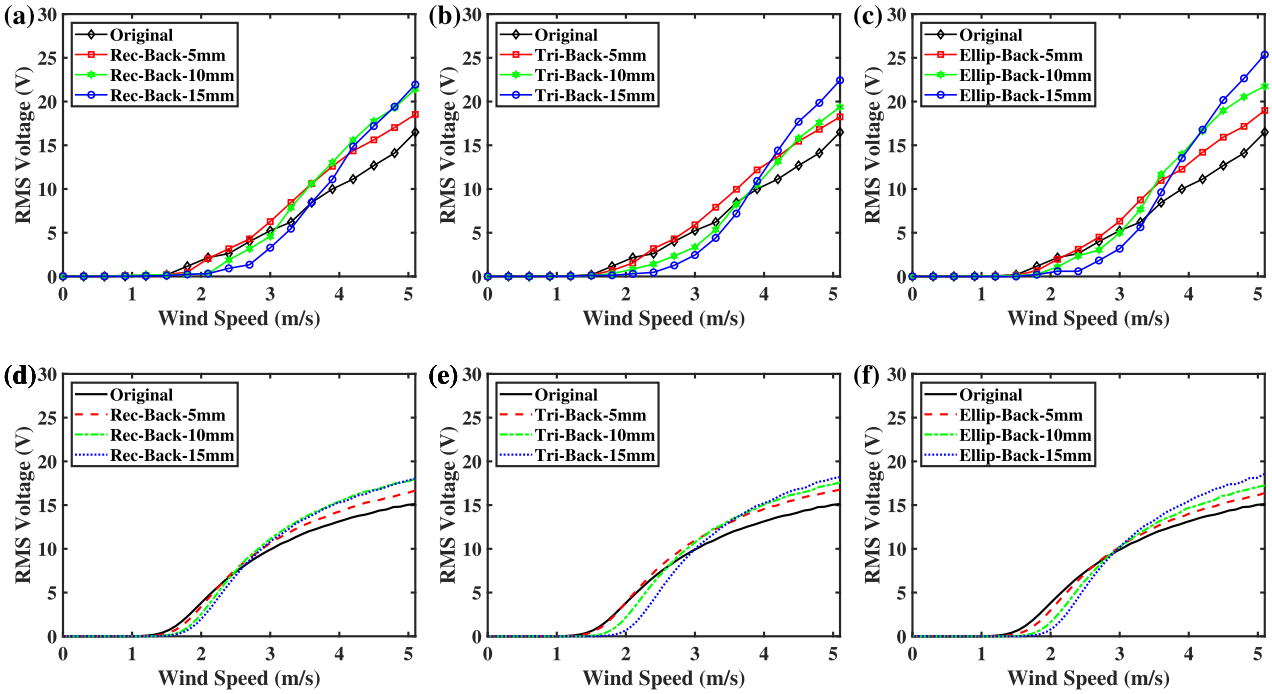

FIG. 3. Experimental RMS output voltage of the bluff bodies with different backward protruded lengths: (a)–(c) with the rectangular, triangular, and elliptical metasurfaces, respectively; and corresponding simulation results: (d)–(f) for the rectangular, triangular, and elliptical metasurfaces, respectively.

$$\alpha = \frac{\left(\dot{w}_{L_b} + \frac{D_b}{2}\dot{w}'_{L_b}\right)}{U_f}, \tag{4}$$

C_{Fy} is also a function of the beam tip deflection.

According to the Den Hartog criterion,[25] which is expressed in Eq. (5), for a system to undergo galloping oscillations, the initial slope of C_{Fy} vs α curve should be positive. In other words, a positive linear aerodynamic coefficient (A_1) is an essential prerequisite for the occurrence of galloping instability, otherwise the GPEH cannot oscillate. Therefore, investigating C_{Fy} behavior can also be beneficial for analyzing the experimental results. Moreover, using the curve fitting method, it can be further expressed explicitly with respect to the AoA in the expression of galloping aeroelastic force. Thus, the governing equations [Eq. (1)] can be solved numerically using MATLAB by the Runge–Kutta method,

$$\left.\frac{dC_{F_y}}{d\alpha}\right|_{\alpha=0^\circ} = A_1 > 0. \tag{5}$$

Based on the theory of quasi-steady assumption,[26] the values of C_L and C_D at each α in the course of oscillations are the same as the values measured at the same value of α in the static wind tunnel experiments or computational fluid dynamics (CFD) simulations.[21] Hence, in this study, a series of wind tunnel simulations are performed by ANSYS Workbench 18 and the obtained results are shown in Fig. 4. It can be observed that for all backward cases, whatever their protruded shape and length are, the initial slope is positive, which implies the occurrence of galloping. However, for all the side and all-sided cases, no matter what the protruded shape is, the initial slope is negative or nearly zero, which means that the system cannot vibrate in a galloping mode. It is interesting to note that for the frontal cases, the triangular and elliptical protruded shapes have positive slopes, but the rectangular shape does not. This indicates that the rectangular frontal protrusions cannot render galloping oscillations, but the other two shapes are able to render. Moreover, according to the previous research conducted by Hu *et al.*,[27,28] the larger the peak value of the C_{Fy} and the α corresponding to $C_{Fy} = 0$, the greater the galloping response. Therefore, the trends in Figs. 4(d)–4(f) suggest a greater response for the bluff bodies with a larger backward protruded length. Most importantly, the above analysis from the wind tunnel CFD simulations is in agreement with the experimental findings of Fig. 2, which in turn proves the validity of the quasi-steady assumption applied in this study.

Using the third-order polynomial curve fitting method, the linear (A_1) and cubic (A_3) aerodynamic coefficients for the galloping cases are obtained and listed in Table I. It can be observed that both A_1 and A_3 increase by increasing the backward protruded length. According to the theory of Parkinson,[29] this is due to the fact that the shear layer, which has separated from one of the upstream corners of the bluff body, reattaches to one of the downstream corners at a larger angle of attack α. However, by comparing them, there seems to be an increasing convergence of both A_1 and A_3 in the rectangular case as the protruded length is increased from 10 to 15 mm. This also implies a convergence of the dynamic response as shown in Figs. 3(a) and 3(d). Corresponding numerical simulations can be performed by substituting each pair of the aerodynamic coefficients into the governing equations. Using this, the simulated results of the RMS voltage are plotted

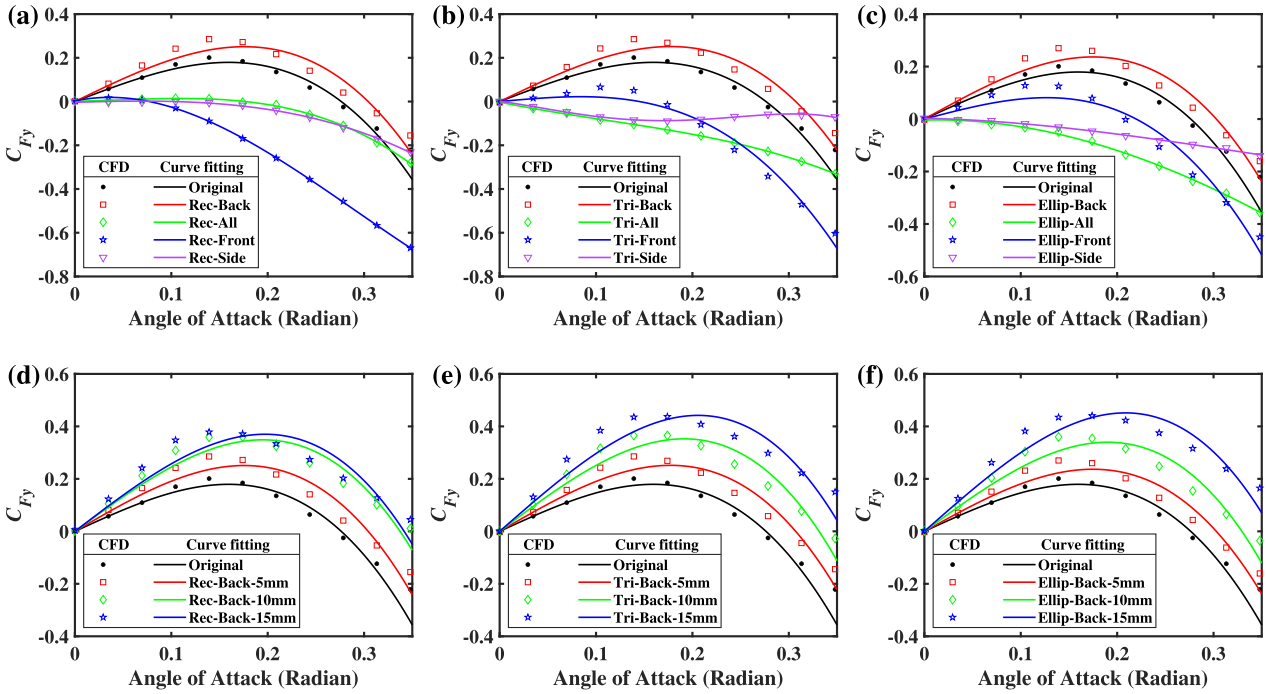

FIG. 4. Diagram of the transverse force coefficient C_{Fy} vs the angle of attack for different protruded bluff bodies: (a)–(c) rectangular, triangular, and elliptical metasurfaces with four types of surface treatments (backward, all-sided, frontal, and side); (d)–(f) rectangular, triangular, and elliptical metasurfaces with three different backward protruded lengths (5/10/15 mm).

in Figs. 3(d)–3(f). It can be seen that the established modeling can well predict the galloping response, especially the cut-in wind speed and its variance in different cases. However, after the cut-in wind speed, there is an over-prediction of the output voltage at lower speeds (2–4 m/s), and an under-prediction at higher speeds (4–5.1 m/s). This discrepancy is probably due to the fact that the wind tunnel CFD simulations normally cannot be absolutely accurate, which leads to some errors in predicting the actual galloping force. Next, the underlying reason for the slight increase in the cut-in wind speed with the increase in the backward protrusion length, which is observed in Fig. 3, is discussed.

TABLE I. Linear and cubic aerodynamic coefficients under third-order polynomial curve fitting approximation.

	A_1	A_3
Original	1.685	22.07
Rec-5	2.142	23.14
Rec-10	2.687	23.62
Rec-15	2.815	24.13
Tri-5	2.128	22.56
Tri-10	2.764	25.17
Tri-15	3.219	25.30
Ellip-5	2.030	22.13
Ellip-10	2.679	24.69
Ellip-15	3.246	24.86

According to Eq. (6), which is obtained by assuming the equivalent linear damping equal to be zero,[25,26] the cut-in speed is proportional to the dimensional viscous damping (c) and inversely proportional to the linear aerodynamic coefficient. Therefore, although increasing the backward protruded length leads to an increased A_1, the ratio of c/A_1 determines the variation of cut-in wind speed with protruded length. After conducting vibration tests on GPEHs with different protruded lengths, it was observed that the ratio of c/A_1 increases by increasing the protruded length. These observations justify the slight increase in cut-in wind speed with increasing protruded length,

$$U_{cut-in} \propto \frac{2c}{\rho L D_b A_1}. \tag{6}$$

Further experiments are conducted to investigate the optimal resistance for each galloping energy harvester. Since the working wind speed is not constant, its influence on the optimal resistance should be considered first. As shown in Fig. 5(a), three different wind speeds are selected for the impedance matching tests of the original bluff body. Results prove that wind speed has a small effect on the optimal resistance for an identical bluff body. Therefore, a single wind speed of 5.1 m/s is selected for the subsequent experiments. Results of Figs. 5(b)–5(d) reveal that for each different protruded bluff body, the optimal resistance is nearly the same, which is around 300 kΩ. As a result, 300 kΩ will be chosen as the load resistance for each GPEH. The GPEH output power vs wind speed for the rectangular/triangular/elliptical bluff bodies is depicted in Figs. 5(e)–5(g). It can be seen that for each backward protruded case, the energy harvesting performance

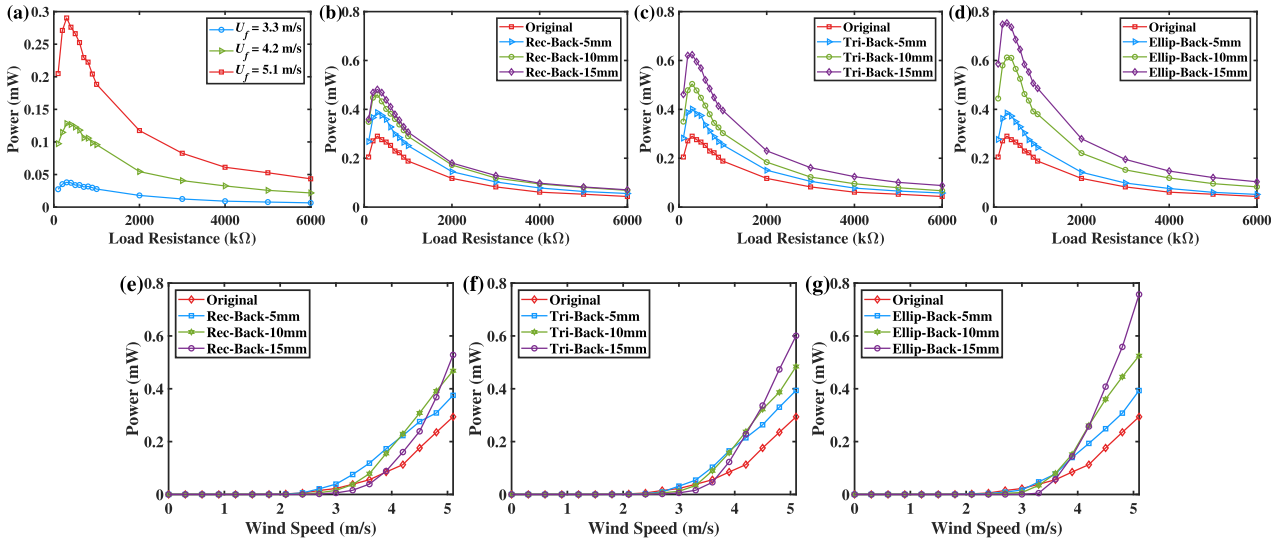

FIG. 5. Experimental results of impedance matching tests: (a) original bluff body under three different wind speeds; (b)–(d) rectangular, triangular, and elliptical backward protruded bluff bodies under the wind speed of 5.1 m/s; (e)–(g) output power under the optimal load resistance of 300 kΩ for different backward protruded bluff bodies.

outperforms the original one when the wind speed is higher than the cut-in speed; with the increase in the protruded length, the harvested energy at the highest studied wind speed also increases. Moreover, the highest output power for the rectangular/triangular/elliptical backward protruded bluff bodies is, respectively, 0.528, 0.601, and 0.757 mW. Hence, compared to 0.294 mW of the original bluff body, the power corresponding to the rectangular/triangular/elliptical backward protruded bluff bodies is enhanced by 79.59%, 104.42%, and 157.48%, respectively. Therefore, it can be concluded that the elliptical surface protrusion with the 15 mm backward protruded length can provide the highest energy harvesting enhancement for the GPEH, which is the desired optimal protrusion shape in this study. It is interesting to note that, unlike the rectangular surface protrusion, which has a clear enhancement convergence when the protruded length reaches 10 mm, there is still a big potential for further output power improvement by increasing the elliptical backward protruded length. Therefore, future work will be focused on finding the optimal solution for this case.

In summary, this Letter explores the potential effect of different surface protrusions on galloping energy harvesting performance. It proves that adding protrusions on the bluff body can obviously change the amplitude and mode of oscillations, and only the backward protrusions are able to enhance the galloping vibration amplitudes, which is a remarkable finding of this study. However, the galloping cut-in speed is increased slightly as the protruded length increases. Wind tunnel CFD simulations were performed to investigate the transverse force coefficients, which can be used to justify the phenomenon observed in the experiments according to the classic Den Hartog's criterion. Both the experiments and numerical simulations show that elliptical surface protrusions have the greatest potential in enhancing galloping energy harvesting performance. With a backward protruded length of 15 mm, the optimum harvested power is experimentally measured to be 0.757 mW at the optimal resistance of 300 kΩ and a wind speed of 5.1 m/s, which outperforms the system carrying the original bluff body by 157.48%. This study demonstrates that by integrating the square prism with optimally designed backward protrusions, the modified galloping energy harvester has a great potential to serve as a sustainable energy source for low-power electronic devices. In the future, advanced optimization methods, such as topology optimizations,[30,31] can be utilized to optimize the backward protrusion shapes and protruded lengths for galloping energy harvesting enhancement.

See the supplementary material for the video demo when the proposed protruded GPEH undergoes the limit-cycle oscillation.

This work was supported by the Hong Kong Innovation and Technology Commission (Project No. MRP/030/21), the Chinese University of Hong Kong (Project ID: 4055178), and the National Natural Science Foundation of China (Grant No. 12202151).

AUTHOR DECLARATIONS

Conflict of Interest

The authors have no conflicts to disclose.

Author Contributions

Juntong Xing: Conceptualization (equal); Data curation (equal); Formal analysis (equal); Investigation (equal); Methodology (equal); Software (equal); Validation (equal); Visualization (equal); Writing – original draft (equal). **Masoud Rezaei:** Conceptualization (equal); Data curation (equal); Formal analysis (equal); Investigation (equal); Methodology (equal); Validation (equal); Writing – review & editing (equal). **HuLiang Dai:** Funding acquisition (equal); Resources (equal); Supervision (equal); Writing – review & editing (equal). **Wei-Hsin Liao:** Funding acquisition (equal); Project administration (equal); Resources (equal); Supervision (equal); Writing – review & editing (equal).

DATA AVAILABILITY

The data that support the findings of this study are available from the corresponding author upon reasonable request.

REFERENCES

[1]J. Wang, D. Yurchenko, G. Hu, L. Zhao, L. Tang, and Y. Yang, "Perspectives in flow-induced vibration energy harvesting," Appl. Phys. Lett. **119**, 100502 (2021).

[2]D. Li, Y. Wu, A. Da Ronch, and J. Xiang, "Energy harvesting by means of flow-induced vibrations on aerospace vehicles," Prog. Aerosp. Sci. **86**, 28–62 (2016).

[3]A. Abdelkefi, "Aeroelastic energy harvesting: A review," Int. J. Eng. Sci. **100**, 112–135 (2016).

[4]F.-R. Liu, H.-X. Zou, W.-M. Zhang, Z.-K. Peng, and G. Meng, "Y-type three-blade bluff body for wind energy harvesting," Appl. Phys. Lett. **112**, 233903 (2018).

[5]A. H. Alhadidi and M. Daqaq, "A broadband bi-stable flow energy harvester based on the wake-galloping phenomenon," Appl. Phys. Lett. **109**, 033904 (2016).

[6]J. Dias, C. De Marqui, Jr., and A. Erturk, "Hybrid piezoelectric-inductive flow energy harvesting and dimensionless electroaeroelastic analysis for scaling," Appl. Phys. Lett. **102**, 044101 (2013).

[7]M. Rezaei and R. Talebitooti, "Wideband PZT energy harvesting from the wake of a bluff body in varying flow speeds," Int. J. Mech. Sci. **163**, 105135 (2019).

[8]K. Yang, J. Wang, and D. Yurchenko, "A double-beam piezo-magneto-elastic wind energy harvester for improving the galloping-based energy harvesting," Appl. Phys. Lett. **115**, 193901 (2019).

[9]J. Xing, S. Fang, X. Fu, and W.-H. Liao, "A rotational hybrid energy harvester utilizing bistability for low-frequency applications: Modelling and experimental validation," Int. J. Mech. Sci. **222**, 107235 (2022).

[10]G. Xu, J. Fu, C. Li, J. Xing, C. Chen, W.-H. Liao, Z. Wang, and Y. Zi, "A nonlinear triboelectric nanogenerator with a broadened bandwidth for effective harvesting of vibration energy," iEnergy **1**, 236–242 (2022).

[11]A. Bibo, A. Abdelkefi, and M. F. Daqaq, "Modeling and characterization of a piezoelectric energy harvester under combined aerodynamic and base excitations," J. Vib. Acoust. **137**, 031017 (2015).

[12]L. Zhang, H. Dai, A. Abdelkefi, and L. Wang, "Improving the performance of aeroelastic energy harvesters by an interference cylinder," Appl. Phys. Lett. **111**, 073904 (2017).

[13]L. Zhang, H. Dai, A. Abdelkefi, and L. Wang, "Experimental investigation of aerodynamic energy harvester with different interference cylinder cross-sections," Energy **167**, 970–981 (2019).

[14]M. Rezaei and R. Talebitooti, "Effects of higher-order terms in aerodynamic force on the nonlinear response of a galloping PZT energy harvester," J. Theor. Appl. Vib. Acoust. **6**, 271–280 (2020).

[15]A. H. Alhadidi, H. Alhussein, and M. F. Daqaq, "Improving the sensitivity of galloping energy harvesters to flow fluctuations," Appl. Phys. Lett. **116**, 263902 (2020).

[16]M. Z. Abdehvand, S. A. S. Roknizadeh, and H. Mohammad-Sedighi, "Modeling and analysis of novel coupled magneto-electro-aeroelastic continuous system for flutter-based energy harvesting system," Energy **230**, 120742 (2021).

[17]Y. Yang, L. Zhao, and L. Tang, "Comparative study of tip cross-sections for efficient galloping energy harvesting," Appl. Phys. Lett. **102**, 064105 (2013).

[18]G. Hu, K.-T. Tse, and K. C. Kwok, "Enhanced performance of wind energy harvester by aerodynamic treatment of a square prism," Appl. Phys. Lett. **108**, 123901 (2016).

[19]J. Wang, S. Sun, L. Tang, G. Hu, and J. Liang, "On the use of metasurface for vortex-induced vibration suppression or energy harvesting," Energy Convers. Manage. **235**, 113991 (2021).

[20]B. Tang, X. Fan, J. Wang, and W. Tan, "Energy harvesting from flow-induced vibrations enhanced by meta-surface structure under elastic interference," Int. J. Mech. Sci. **236**, 107749 (2022).

[21]J. Wang, S. Sun, G. Hu, Y. Yang, L. Tang, P. Li, and G. Zhang, "Exploring the potential benefits of using metasurface for galloping energy harvesting," Energy Convers. Manage. **243**, 114414 (2021).

[22]T. Tan, L. Zuo, and Z. Yan, "Environment coupled piezoelectric galloping wind energy harvesting," Sens. Actuators, A **323**, 112641 (2021).

[23]M. Rezaei, R. Talebitooti, W.-H. Liao, and M. I. Friswell, "Integrating PZT layer with tuned mass damper for simultaneous vibration suppression and energy harvesting considering exciter dynamics: An analytical and experimental study," J. Sound Vib. **546**, 117413 (2023).

[24]M. Rezaei, S. E. Khadem, and P. Firoozy, "Broadband and tunable PZT energy harvesting utilizing local nonlinearity and tip mass effects," Int. J. Eng. Sci. **118**, 1–15 (2017).

[25]J. P. Den Hartog, *Mechanical Vibrations* (Courier Corporation, 1985).

[26]M. P. Païdoussis, S. J. Price, and E. De Langre, *Fluid-Structure Interactions: Cross-Flow-Induced Instabilities* (Cambridge University Press, 2010).

[27]G. Hu, K. T. Tse, M. Wei, R. Naseer, A. Abdelkefi, and K. C. Kwok, "Experimental investigation on the efficiency of circular cylinder-based wind energy harvester with different rod-shaped attachments," Appl. Energy **226**, 682–689 (2018).

[28]G. Hu, K.-T. Tse, and K. C. Kwok, "Galloping of forward and backward inclined slender square cylinders," J. Wind Eng. Ind. Aerodyn. **142**, 232–245 (2015).

[29]G. Parkinson, "Wind-induced instability of structures," Philos. Trans. R. Soc. London., Ser. A **269**, 395–413 (1971).

[30]O. Sigmund and K. Maute, "Topology optimization approaches," Struct. Multidisc. Optim. **48**, 1031–1055 (2013).

[31]S. Boyd, S. P. Boyd, and L. Vandenberghe, *Convex Optimization* (Cambridge University Press, 2004).